Observing transiting exoplanets with JWST/NIRSpec

Ferruit P.[a], Birkmann S.[b], Böker T.[b], Sirianni M.[b], Giardino G.[a], de Marchi G.[a], Alves de Oliveira C.[c] and Dorner B.[d]

[a] European Space Agency / ESTEC, Keplerlaan 1, 2201 AZ Noordwijk, The Netherlands;
[b] European Space Agency / STScI, 3700 San Martin Dr, Baltimore, MD 21218, United States;
[c] European Space Agency / ESAC, Camino Bajo del Castillo, s/n., Urb. Villafranca del Castillo, 28692 Villanueva de la Cañada, Madrid, Spain;
[d] Max Planck Institute for Astronomy, Königstuhl 17, 69117 Heidelberg, Germany.

ABSTRACT

Recent publications resulting from observations conducted with the Hubble Space Telescope (HST) have highlighted the diagnostic power of near-infrared spectroscopy for the study of the atmospheric properties of transiting exoplanets. In this context, the James Webb Space Telescope (JWST) and it suite of instruments will have an unprecedented combination of sensitivity and spectral coverage. In this article, we focus on one of these instruments, the near-infrared spectrograph NIRSpec. NIRSpec will offer an aperture spectroscopy mode dedicated to the characterization of transiting exoplanets. It will cover the 0.6-5.3 μm spectral domain with 3 ranges of spectral resolution (R 100, 1000 and 2700). The predicted noise floor (photon noise and detector noise only, no systematics included) is lower than 100 ppm for a single 1-hour in-transit observation of an 7^{th} magnitude star, indicating that transit spectroscopy programs with NIRSpec will routinely have photon-noise limited noise floors of a few tens of ppm. In terms of brightness limits, at high spectral resolution, NIRSpec will be able to observe planets transiting stars with J-band magnitudes up to 6.5 in the worst case and 4.5 in the best case.

Keywords: JWST, NIRSpec, infrared, spectroscopy, transit, exoplanets

1. INTRODUCTION

The diagnostic power of near-infrared spectroscopy for the study of the atmospheric properties of transiting exoplanets has recently been put under the spotlight by several studies conducted with the Hubble Space Telescope (HST; see e.g. Kreidberg et al.[1]). In this context, the near-infrared spectrograph NIRSpec (Birkmann et al.[2]), on board the James Webb Space Telescope (JWST; Gardner et al.[3]) will offer a very attractive set of capabilities to the JWST users.

NIRSpec is a near-infrared spectrograph capable of low- (R$\sim$ 100), medium- (R$\sim$ 1000) and high- (R$\sim$ 2700) resolution spectroscopy between 0.6 and 5.3 μm. It can be operated in three different modes: multi-object spectroscopy (MOS mode) over an area of 9 square arcminutes with micro-shutter arrays for the selection of the sources; integral field spectroscopy (IFU mode) over a field of view of 3"$\times$3" and with a sampling of 0.1"; and slit spectroscopy (SLIT mode) using five high-contrast slits.

One of these five slits is, in fact, a square 1.6"$\times$1.6" aperture designed specifically for exoplanet transit spectroscopy, and it will serve as the primary mode for observing exoplanets with NIRSpec. The combination of wavelength coverage and spectral resolution provided by NIRSpec will make it possible to resolve spectral features of many molecules expected to be found in exoplanet atmospheres, allowing to put constraints on their elemental abundances and thermal structures.

In this paper, we will first detail the capabilities of the instrument's aperture spectroscopy mode. We will then describe its expected performances in the context of transit spectroscopy of exoplanets.

Space Telescopes and Instrumentation 2014: Optical, Infrared, and Millimeter Wave, edited by Jacobus M. Oschmann, Jr., Mark Clampin, Giovanni G. Fazio, Howard A. MacEwen, Proc. of SPIE Vol. 9143, 91430A · © 2014 SPIE
CCC code: 0277-786X/14/$18 · doi: 10.1117/12.2054756

2. NIRSPEC CAPABILITIES

2.1 NIRSpec Configurations for Exoplanet Transit Spectroscopy

A summary of the characteristics of the spectral configurations of NIRSpec available for transit spectroscopy with the SLIT/A1600 aperture is provided in Table 1, while a plot of the associated spectral resolution curves can be found in Figure 1. Note that these curves correspond to the case of a fully illuminated 200-mas slit (yielding a spectral PSF width of roughly 2.0-2.2 detector pixels). In the case of the wide SLIT/A1600 aperture, the shape of the spectral PSF will not be defined by the shape of the illuminated slit, but by the spatial PSF itself. Simulations have shown that in this case, although the spectral PSF will exhibit a narrow undersampled core with sizes ranging from 0.5 to 1.5 detector pixels (increasing with wavelength), its typical width yields spectral resolution values consistent with those displayed in Figure 1.

Using the CLEAR/PRISM configuration, the complete near-infrared spectral range (0.6-5.3 μm) can be covered at low spectral resolution (typically 30-300, see Figure 1) with a single exposure. This configuration has no equivalent in the other *JWST* near-infrared instruments. It also provides some wavelength overlap with the MIRI LRS configuration, opening the possibility to "stitch" NIRSpec and MIRI spectra together.

NIRSpec transit spectroscopy				
Instrument mode		SLIT/A1600		
Aperture size (projected on the sky)		1.6"×1.6"		
Aperture size (projected on the detectors)		∼16×16 pixels		
				Low spectral resolution spectroscopy (R∼100)
Wavelength range:				from 0.6 μm to 5.3 μm in a single band
Spectral resolution:				30-300
Instrument configuration:				CLEAR/PRISM
Readout subarray size:				512×32 pixels (spectral × spatial)
Frame readout time:				0.226 s (single frame)
				Medium spectral resolution spectroscopy (R∼1000)
Instrument configuration:	Range	Resolution	Readout subarray size	Frame readout time
F070LP/G140M	[0.7μm, 1.2μm]	500-850	2048×32 pixels	0.902 s
F100LP/G140M	[1.0μm, 1.8μm]	700-1300	2048×32 pixels	0.902 s
F170LP/G235M	[1.7μm, 3.1μm]	700-1300	2048×32 pixels	0.902 s
F290LP/G395M	[2.9μm, 5.2μm]	700-1300	2048×32 pixels	0.902 s
				High spectral resolution spectroscopy (R∼2700)
Instrument configuration:	Range	Resolution	Readout subarray size	Frame readout time
F070LP/G140H	[0.7μm, 1.2μm]	1300-2300	2048×32 pixels	0.902 s
F100LP/G140H	[1.0μm, 1.8μm]	1900-3600	2048×32 pixels	0.902 s
F170LP/G235H	[1.7μm, 3.1μm]	1900-3600	2048×32 pixels	0.902 s
F290LP/G395H	[2.9μm, 5.2μm]	1900-3600	2048×32 pixels	0.902 s

Table 1. Characteristics of the NIRSpec SLIT/A1600 mode for transit spectroscopy.

At higher spectral resolution, NIRSpec is using gratings as dispersers and, to prevent order overlap, it is necessary to use 3 (4) different spectral configurations to cover the 1.0-5.2 (0.7-5.2) μm range. The extension of the wavelength coverage below 1.0 μ is obtained using the G140M/H gratings outside of their nominal wavelength range and it will be associated with a drop in the photon conversion efficiency as one moves further and further away from the peak of the grating blaze function.

2.2 Operating the NIRSpec Detectors for Transit Spectroscopy

In the case of transit spectroscopy, it is advantageous (in terms of final signal to noise ratio) to accumulate as many photons as possible from the host star. As a consequence, for transiting planets of similar scientific interest, the one orbiting the brightest host star will usually be favored. It is therefore important for NIRSpec to be able to observe stars as bright as possible and to do it in the most efficient manner. In this context, the way NIRSpec's detectors are operated is key to the final performance and operational efficiency of the instrument.

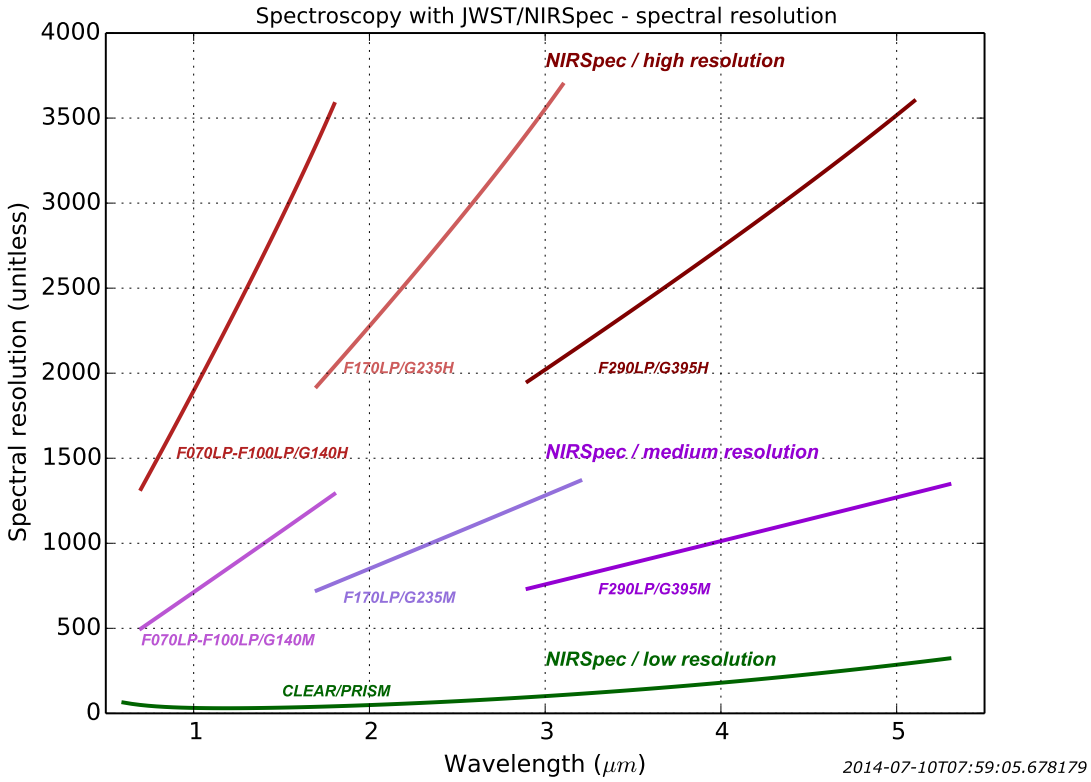

Figure 1. Spectral resolution curves as a function of wavelength for the various spectral configurations of JWST/NIRSpec

NIRSpec's detector system (Rauscher et al.[4]) includes two H2RG HgCdTe detectors (2048×2048 arrays) and two application-specific integrated circuits (ASICs). In the following subsection, we describe relevant aspects of their performances and operation.

2.2.1 Saturation Limits

NIRSpec's detectors have been optimized for the observation of faint objects in a low background environment. Their system gain (in electrons per analog-to-digital units [ADU]) has therefore been adjusted to provide a good sampling of the noise level and not to ensure a complete coverage of the full well. As a consequence, saturation is not defined by the full-well capacity but is set by the 16-bits of the analog-to-digital converter. For a typical gain of 1.2 electrons per ADU, this yields a saturation limit of 77000 electrons. The possibility to have a dedicated system gain setting for transit spectroscopy is currently being discussed, but as this has not yet been baselined, we will use a limit of 77000 electrons throughout this paper.

Note that tests have also been conducted both at STScI (M. Regan) and at GSFC (B. Rauscher) to evaluate the possibility of having a dedicated observing mode with an increased detector reverse bias level, aiming at roughly doubling the full-well capacity ("bright object" mode to be contrasted with the baseline "faint object" one). Although the detectors were shown to exhibit good performances in this mode, it was found that transiting between the bright and faint modes triggered strong persistence over a period of several hours. This was not acceptable from an operational point of view, and this option therefore has not been baselined.

2.2.2 Subarrays

Another important parameter for the observation of bright targets is the time needed to read the detectors. In NIRSpec's SLIT/A1600 mode, the spectrum of the source covers only a small fraction of the detectors and

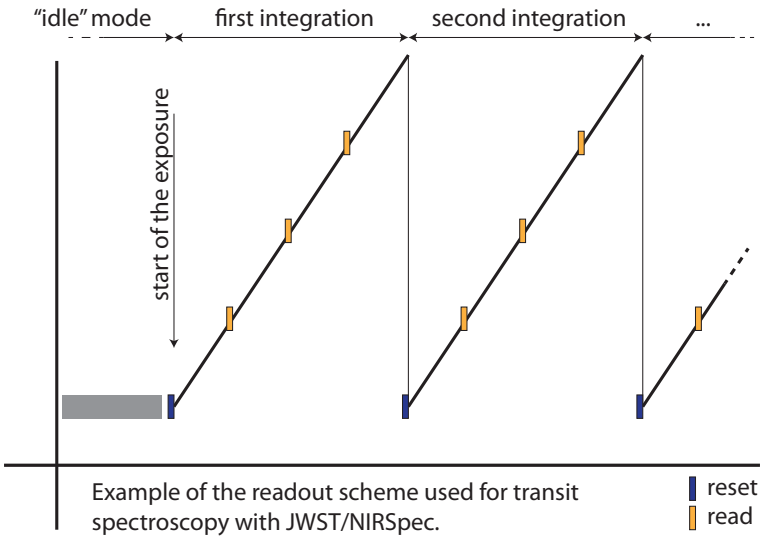

Figure 2. Readout scheme used for transit spectroscopy with NIRSpec.

subarrays will be used (WINDOW mode). The subarray sizes and the associated frame readout times are listed in Table 1. They correspond to the minimum possible sizes that adhere to two important constraints: the size of each subarray dimension must be a power of two, and the subarray must be large enough (dispersion direction $\times$ spatial direction) to include the complete spectrum (accounting for any spectral curvature due to distortion). In the case of the low spectral resolution CLEAR/PRISM configuration, the spectra are short and this allows one to use a fairly short subarray (512 pixels along the dispersion direction). The frame readout times in Table 1 can be compared to the 10.74 s needed to read the full detector using four outputs in parallel (FULL-FRAME mode). Note that only one output is used when reading out subarrays.

2.2.3 Readout scheme

The baseline readout mode used for JWST's near-infrared instruments, an up-the-ramp readout scheme called MULTIACCUM (see Rauscher et al.[5]), is very versatile and its parameters can be adapted to suit the specific needs of transit spectroscopy. The observation of a transit will consist of one or more exposures containing up to 65535 integrations. Each integration will start with a reset (fast row-by-row reset of the full array followed by a pixel-to-pixel reset of the subarray) followed by a user-defined number of non-destructive frame readouts (see sketch in Figure 2). Note that although a solution where at least two frames are read per integration (reset-read-read-...) is usually preferred, for very bright sources it is possible to obtain integrations with a single frame readout (reset-read). In this case special attention has to be payed to the subtraction of the initial reset levels.

Note that between the exposures, the NIRSpec detectors return to the so-called "idle-mode" where the four outputs are used instead of a single one in WINDOW mode. This will change significantly the dissipation in the ASICs and may introduce some instabilities in the system. As a consequence, it is advised to add more integrations, rather than using multiple exposures. Assuming the shortest possible integration (reset-read) and the maximum number of integrations per exposure (65535), a single exposure will already be able cover more than 9 hours for a 512×32 subarray and 33 hours for a 2048×32 subarray.

3. EXPECTED PERFORMANCES

3.1 Photon Conversion Efficiency

The key ingredient for estimating the expected saturation and sensitivity limits for NIRSpec in a given configuration is its photon conversion efficiency (PCE hereafter). The PCE of NIRSpec has been evaluated during one of the NIRSpec-level cryogenic test campaign in early 2013. These tests showed that the PCE curves derived from an extensive set of sub-system level measurements were conservative but consistent with the NIRSpec level

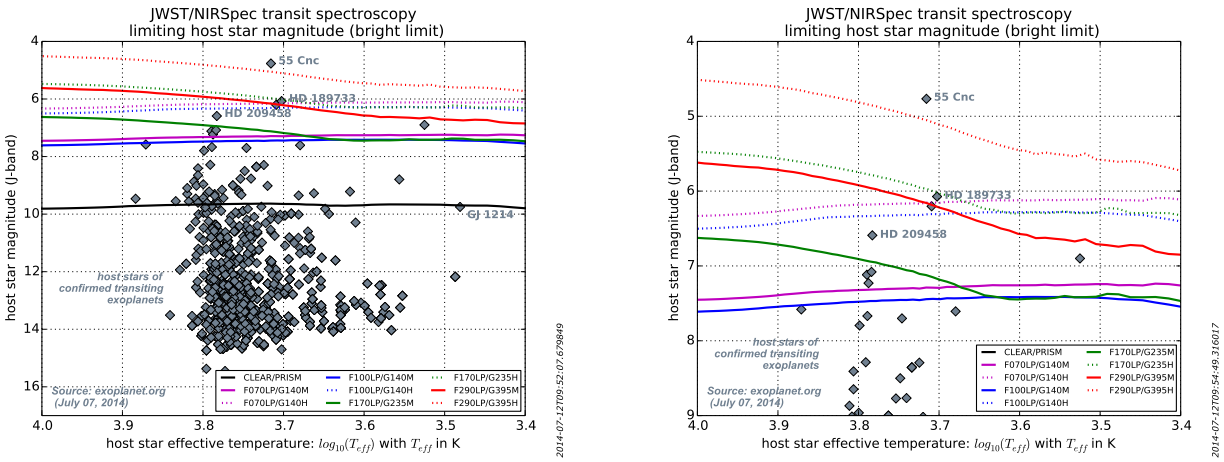

Figure 3. Upper limit on the brightness of the host star (in J-band magnitude) as a function of the effective temperature of the host star and for the various NIRSpec configurations. The symbols denote the host stars of all confirmed transiting exoplanets, obtained from the site exoplanet.org (as of the 7^{th} of July 2014). The right panel is a zoomed version of the left one. We remind the reader that our estimates have uncertainties of typically 20 % (i.e. 0.2 magnitudes)

measurements and they will therefore form the basis of the computation results presented in this paper. **We emphasize that there are strong uncertainties (typically of the order of 20 %) on these PCE curves and that this should not be forgotten when using the results presented in this paper.**

The notion of a "conservative" PCE curve can have completely different interpretations, depending on wether it is used to compute a saturation limit or a sensitivity limit. We therefore modified the PCE curves in the following ways:

- For the computation of saturation limits, we used PCE estimates corresponding to the "beginning of life" of the instrument, i.e. immediately after commissioning and when the PCE will be the highest.
- For the computation of sensitivity limits and signal to noise ratios, we used "end-of-life" PCE estimates that include a flat degradation of 10 % compared to the "beginning-of-life" ones.

The PCE curves include the transmission of the JWST telescope optics, and for these we used a typical gold coating curve normalized to match the requirements on the telescope transmission.

3.2 Saturation Limits

As already highlighted in section 2.2, the best targets for studies of the atmospheres of transiting exoplanets will likely be bright host stars, and it will be important to know whether they can indeed be observed with NIRSpec without saturating the detectors. We have therefore computed the limiting host star magnitude as a function of the host star effective temperature for the various spectral configurations offered by NIRSpec. The computation has been performed using the PCE described in section 3.1, assuming the shortest possible integration (reset-read, see section 2.2.3) and a saturation limit of 77000 electrons (see section 2.2.1). For the spectrum of the host star, we used stellar spectra from models computed using the Phoenix code by F. Allard and collaborators (see Allard et al.[6]).

Unsurprisingly, very bright stars cannot be observed at low spectral resolution (CLEAR/PRISM configuration). However, as one can see in Figure 3, there are plenty of potential targets for this mode, which could turn out to be a very powerful candidate screening tool thanks to its extensive wavelength coverage. This brightness limit becomes much less stringent for higher spectral resolution configurations. The worst case saturation limits correspond to J-band magnitudes of 7.5 and 6.5 for the medium and high spectral resolution cases, respectively.

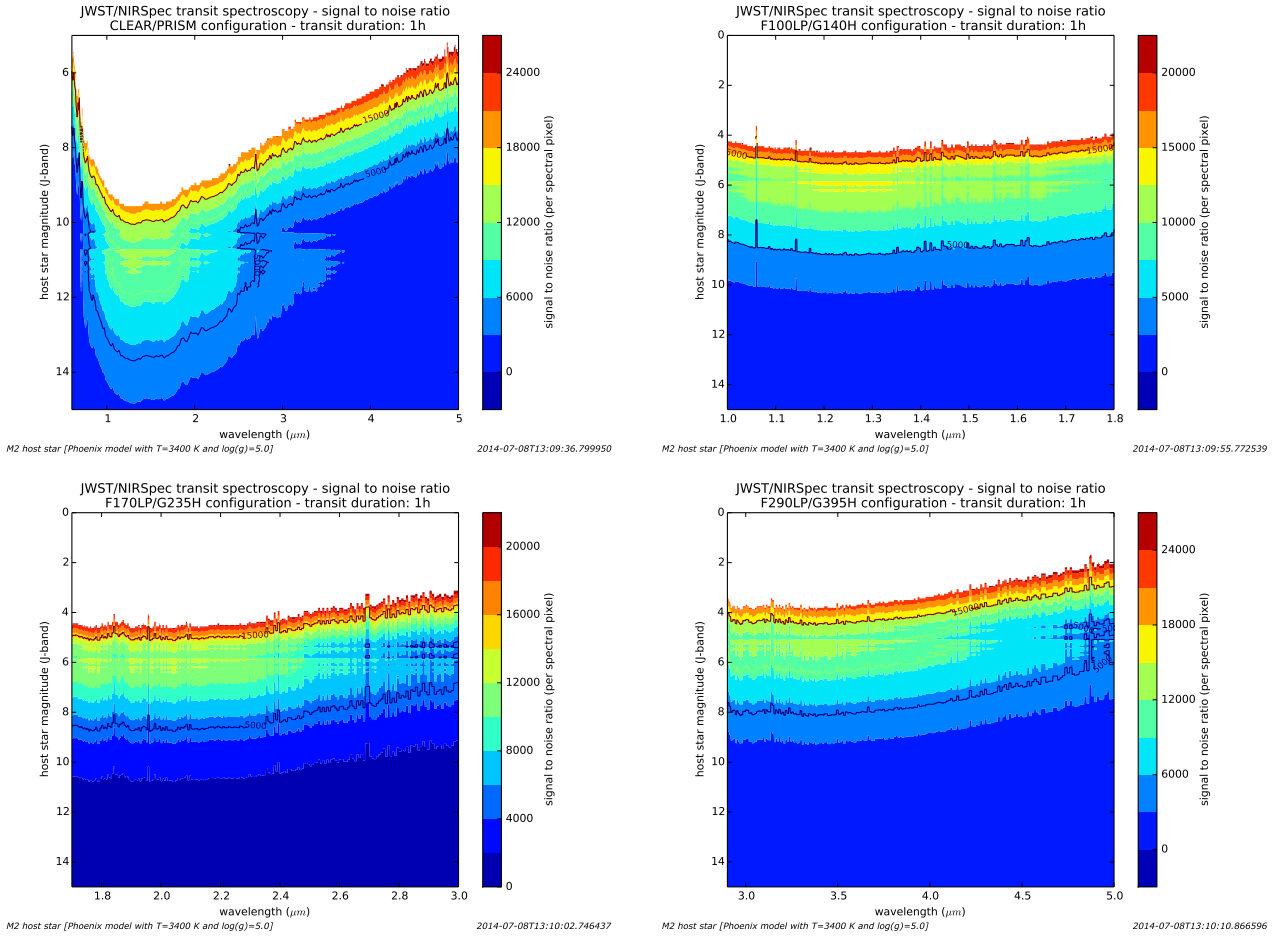

Figure 4. Signal to noise ratio maps as a function of host star magnitude (J band) and wavelength for various configurations and for a 1-h transit observation. Regions where saturation takes place before the first read and that are therefore not usable are indicated in white.

3.3 Sensitivity limits - Benchmark noise floor

To provide a benchmark noise floor for NIRSpec observations, we have computed what would be their signal to noise ratio if only photon and detector noise were present (i.e. no systematics). The computation was performed for the observation of a planet orbiting a M2 host star (effective temperature of 3400 K, Rajpurohit et al.;[7] $log(g) = 5.0$) that would consist of a single "in-transit" exposure of 1 hour (wall-clock time, i.e. including the overheads present in an exposure) combined with two similar "out-of-transit" exposures.

Note that whenever possible, we estimated the signal to noise ratio of the exposures in two different ways corresponding to two different data processing cases:

- By assuming that the processing of the data obtained during an integration would be performed using the difference between the last and the first readouts (*last* - *first*). This is obviously only possible in cases where the saturation was not reached before the second readout. In this case, the signal and the photon noise were computed for the *last-first* difference and the detector noise was for two readouts (readout noise of 18 electrons).

- By assuming that the processing of the data obtained during an integration would be performed using the difference between the last readout and a high signal to noise map of the reset levels (*last* - *reset*). In this

case the signal and the photon noise were computed for the *last-reset* difference while the detector noise was for one readout (18 electrons) and one kTC noise (60 electrons).

When two signal to noise ratio estimates were available, we picked the highest of the two. The resulting plots of the benchmark signal-to-noise ratio (detector and shot noise; no systematics) per spectral pixel for a transit spectroscopy observation as a function of wavelength and the host star J-band magnitude are shown in Figure 4. The excellent sensitivity of JWST/NIRSpec means that the noise floor will be low. As an example, at a spectral resolution of ∼2700 (quite high for any standard of current exoplanet atmospheric studies), only one hour of in-transit observation is necessary to reach a noise floor of 100 parts per million (ppm) per spectral pixel for a 7^{th} magnitude host star (J-band).

3.4 Sensitivity - Systematics

The noise floor values presented in the previous section indicate that transit spectroscopy programs with JWST/NIRSpec will routinely have photon-noise limited noise floors of a few tens of ppm. It is therefore extremely important to eliminate (or calibrate out) any sources of systematic noise that could prevent one from approaching this theoretical limit.

There are many sources of systematic noise that may impact NIRSpec observations of transiting planets. We have listed the obvious major ones in Table 2. It can be seen that the **raw** contribution of one of these, intra-pixel sensitivity variations, is large compared to the targeted noise floor and will need to be removed with careful calibration. The good news is that these systematics are similar to those affecting observations with *HST* and *Spitzer*, so that the analysis techniques honed for current data will provide a good running start for approaching the noise floor for NIRSpec observations.

Noise contribution	Description	Comment
Detector and shot noises	These contribution are included in the baseline simulations and used to estimate the "noise floor".	Used as a benchmark.
Variable aperture losses	The level of aperture losses can change when the source drifts during a transit observation.	**Raw** contribution of typically 40 ppm (B. Dorner, PhD thesis, 2012).
Intra-pixel sensitivity changes	The detector response can change when the source drifts across pixel boundaries during a transit observation.	**Raw** contribution of up to 400 ppm. Major contributor because of the poor PSF sampling in NIRSpec.
Accuracy of the flat-field correction	Another source of detector response change when the source drifts during a transit observation.	Raw impact not yet assessed.
PSF variations	The signal amplitude will change as the footprint of the PSF on the detectors change.	Raw impact not yet assessed.
Persistence	Residual signal changing with time.	Observed in *HST*/WFC3 data (e.g. Berta et al.[8]).

Table 2. List of various noise contributions for the NIRSpec transit spectroscopy.

4. CONCLUSIONS

JWST/NIRSpec will be a powerful tool for the study of the atmospheric properties of transiting exoplanets. It will offer JWST users a very attractive set of capabilities and an unprecedented combination of wavelength coverage, spectral resolution and sensitivity. These will allow to resolve the spectral features of many molecules expected to be found in exoplanet atmospheres, allowing to put constraints on their elemental abundances and thermal structures.

REFERENCES

1. L. Kreidberg, J. L. Bean, J.-M. Désert, B. Benneke, D. Deming, K. B. Stevenson, S. Seager, Z. Berta-Thompson, A. Seifahrt, and D. Homeier, "Clouds in the atmosphere of the super-Earth exoplanet GJ1214b," *Nature* **505**, pp. 69–72, Jan. 2014.
2. S. Birkmann, P. Ferruit, C. Alves de Oliveira, T. Böker, G. de Marchi, G. Giardino, M. Sirianni, M. Stuhlinger, P. Jensen, P. Rumler, M. Falcolini, M. te Plate, G. Cresci, B. Dorner, R. Ehrenwinkler, X. Gnata, and T. Wettemann, "Status of the JWST/NIRSpec instrument," in *Society of Photo-Optical Instrumentation Engineers (SPIE) Conference Series*, *Society of Photo-Optical Instrumentation Engineers (SPIE) Conference Series*, 2014.
3. J. P. Gardner, J. C. Mather, M. Clampin, R. Doyon, M. A. Greenhouse, H. B. Hammel, J. B. Hutchings, P. Jakobsen, S. J. Lilly, K. S. Long, J. I. Lunine, M. J. McCaughrean, M. Mountain, J. Nella, G. H. Rieke, M. J. Rieke, H.-W. Rix, E. P. Smith, G. Sonneborn, M. Stiavelli, H. S. Stockman, R. A. Windhorst, and G. S. Wright, "The James Webb Space Telescope," *Space Science Reviews* **123**, pp. 485–606, Apr. 2006.
4. B. J. Rauscher, D. F. Figer, M. W. Regan, T. Boeker, J. Garnett, R. J. Hill, G. Bagnasco, J. Balleza, R. Barney, L. E. Bergeron, C. Brambora, J. Connelly, R. Derro, M. J. DiPirro, C. Doria-Warner, A. Ericsson, S. D. Glazer, C. Greene, D. N. Hall, S. Jacobson, P. Jakobsen, E. Johnson, S. D. Johnson, C. Krebs, D. J. Krebs, S. D. Lambros, B. Likins, S. Manthripragada, R. J. Martineau, E. C. Morse, S. H. Moseley, D. B. Mott, T. Muench, H. Park, S. Parker, E. J. Polidan, R. Rashford, K. Shakoorzadeh, R. Sharma, P. Strada, A. Waczynski, Y. Wen, S. Wong, J. Yagelowich, and M. Zuray, "Detectors for the James Webb Space Telescope near-infrared spectrograph," in *Optical, Infrared, and Millimeter Space Telescopes*, J. C. Mather, ed., *Society of Photo-Optical Instrumentation Engineers (SPIE) Conference Series* **5487**, pp. 710–726, Oct. 2004.
5. B. J. Rauscher, O. Fox, P. Ferruit, R. J. Hill, A. Waczynski, Y. Wen, W. Xia-Serafino, B. Mott, D. Alexander, C. K. Brambora, R. Derro, C. Engler, M. B. Garrison, T. Johnson, S. S. Manthripragada, J. M. Marsh, C. Marshall, R. J. Martineau, K. B. Shakoorzadeh, D. Wilson, W. D. Roher, M. Smith, C. Cabelli, J. Garnett, M. Loose, S. Wong-Anglin, M. Zandian, E. Cheng, T. Ellis, B. Howe, M. Jurado, G. Lee, J. Nieznanski, P. Wallis, J. York, M. W. Regan, D. N. B. Hall, K. W. Hodapp, T. Böker, G. De Marchi, P. Jakobsen, and P. Strada, "Detectors for the James Webb Space Telescope Near-Infrared Spectrograph. I. Readout Mode, Noise Model, and Calibration Considerations," *PASP* **119**, pp. 768–786, July 2007.
6. F. Allard, D. Homeier, and B. Freytag, "Model Atmospheres From Very Low Mass Stars to Brown Dwarfs," in *16th Cambridge Workshop on Cool Stars, Stellar Systems, and the Sun*, C. Johns-Krull, M. K. Browning, and A. A. West, eds., *Astronomical Society of the Pacific Conference Series* **448**, p. 91, Dec. 2011.
7. A. S. Rajpurohit, C. Reylé, F. Allard, R.-D. Scholz, D. Homeier, M. Schultheis, and A. Bayo, "High-resolution spectroscopic atlas of M subdwarfs. Effective temperature and metallicity," *A&A* **564**, p. A90, Apr. 2014.
8. Z. K. Berta, D. Charbonneau, J.-M. Désert, E. Miller-Ricci Kempton, P. R. McCullough, C. J. Burke, J. J. Fortney, J. Irwin, P. Nutzman, and D. Homeier, "The Flat Transmission Spectrum of the Super-Earth GJ1214b from Wide Field Camera 3 on the Hubble Space Telescope," *ApJ* **747**, p. 35, Mar. 2012.